Appl Phys B (2010) 100: 875–881
DOI 10.1007/s00340-010-4105-8

Applied Physics B
Lasers and Optics

Semianalytical theory of plasmon nanoruler

K. Madoyan · A. Melikyan · H. Minassian

Received: 1 December 2009 / Revised version: 29 March 2010 / Published online: 30 June 2010

Abstract We develop a new method based on the continuous-fraction approach as applied to the electrostatic boundary problem for determining surface plasmon resonances of coupled nanospheres. The resonance frequency dependence on interparticle gap (plasmon nanoruler effect) is determined by avoiding time-consuming numerical calculations even for very small interparticle separations, where known procedures face serious difficulties. Corrections due to retardation effects are accounted for, allowing description of larger nanopairs. Good agreement is demonstrated both with results of numerical calculations and with experimental data.

It is well known that for the system of two interacting metallic nanospheres both experimental data and numerical calculations show a strong dependence of surface plasmon (SP) frequencies—ω_{sp} on interparticle center-to-center distance—a [1–13]. This fact opens new possibilities for applications of coupled metallic nanoparticles (MNP) in single-molecule biophysics as nanoscale rulers [2, 13]. The peculiarities in optical properties of nanopairs can be utilized also in optical technologies for chemical or biological imaging and sensing and in surface-enhanced Raman scattering [1, 2, 14, 16]. The spectral shift in the plasmon resonance can be employed to detect specific biomolecules including DNA and protein biomarkers [2].

K. Madoyan · A. Melikyan
Russian–Armenian (Slavonic) State University,
123 Hovsep Emin Str., Yerevan 0051, Armenia

H. Minassian (✉)
Yerevan Physics Institute, after A. Alikhanian,
2 Alikhanian Brothers Str., Yerevan 0036, Armenia
e-mail: hminassian@shen.am

The dependence of SP frequencies on interparticle distance in nanopairs is especially pronounced when $a < 1.1D$ (D is the diameter of the sphere) [11]. For such small distances, however, the various numerical methods employed require enormous volume of calculations that become a serious barrier for obtaining reliable results. To the best of our knowledge the smallest interparticle distances are considered by Shmeits and Dambly [10] and Nordlander et al. [5], where the SP frequency dependence on the interparticle distance down to $1.014D$ and $1.0005D$ correspondingly are calculated numerically. It is important to mention here that all known numerical methods for the calculation of ω_{sp} lead to a cumulative error of several percents which arises as a result of discretization of the volume or the surface of the particles. Large number of parameters of the problem—the characteristics of the metal and the medium in which the particles are placed, the particle sizes etc., create additional complications for calculations. These circumstances suggest the necessity of the development of a new approach allowing the approximate calculation of SP resonances analytically for arbitrary values of the interparticle distances.

Recently a physically clear approximate analytical approach has been developed [17] allowing one to easily obtain SP resonance frequencies of longitudinal and transversal oscillations of a pair of small nanospheres $D \ll \lambda_{sp}/2\pi$. It was demonstrated that for interparticle distances down to $1.05D$ the deviation from the results obtained with use of numerical methods [11] is less than 2%. Accordingly for the mentioned distance scale the "plasmon nanoruler" equation was derived from the electrostatic boundary problem for the first time. It was also shown that the dependence $\omega_{sp}(a)$ is close to exponential. However, for smaller distances (less than $1.05D$) the deviation between the results obtained by numerical simulations and the approximate analytical formula increases. This circumstance indicates the limited va-

lidity of the approach [17] for the case of nearly touching nanospheres.

The calculation of SP resonances of coupled spheres can be realized by use of bispherical coordinates [9, 12] in which the Laplace equation allows the variable separation. This method allowing, in principle, the consideration of smaller interparticle distances obviously requires again a large volume of numerical calculations.

In this paper we present a semianalytical method based on continuous-fraction approach for determining the SP frequencies of nanopairs that radically reduces the calculation time without posing constraints on the value of a/D. It is demonstrated that the developed method for the small size "plasmon nanoruler" provides good agreement with known experimental data.

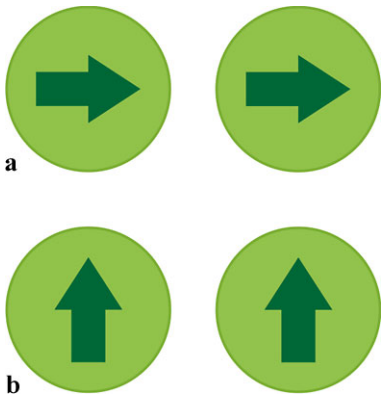

Fig. 1 Arrows show electron cloud displacement for in-phase longitudinal (**a**) and in-phase transversal (**b**) oscillations in the coupled spheres

1 Recurrence equations

When the system size is much smaller than the radiation wavelength of plasma oscillations, the electrostatic approximation is applicable, which allows us to reduce the wave equation to the Laplace equation with corresponding boundary conditions. The procedure of variable separation in Laplace equation developed in the referred articles [9, 12] leads to an infinite recursive relation, which is considered as a system of linear homogeneous equations. The boundary problem for two spheres was considered in bispherical coordinates by R. Ruppin [9], which allowed us to obtain the following system of equations with respect to unknown expansion coefficients A_n for the in-phase longitudinal dipole mode ((12) of [9]).

$$
\begin{aligned}
&n\left[\varepsilon_m \cosh\left(n-\frac{1}{2}\right)\eta_0 + \varepsilon(\omega)\sinh\left(n-\frac{1}{2}\right)\eta_0\right]A_{n-1}\\
&\quad -\sinh\eta_0 \sinh\left(n+\frac{1}{2}\right)\eta_0[\varepsilon_m-\varepsilon(\omega)]A_n\\
&\quad -(2n+1)\cosh\eta_0\left[\varepsilon_m\cosh\left(n+\frac{1}{2}\right)\eta_0\right.\\
&\quad \left.+\varepsilon(\omega)\sinh\left(n+\frac{1}{2}\right)\eta_0\right]A_n\\
&\quad +(n+1)\left[\varepsilon_m\cosh\left(n+\frac{3}{2}\right)\eta_0\right.\\
&\quad \left.+\varepsilon(\omega)\sinh\left(n+\frac{3}{2}\right)\eta_0\right]A_{n+1}=0,
\end{aligned}
\tag{1}
$$

where $\varepsilon(\omega)$ is the dielectric function of the metal, ε_m is the dielectric constant of the surrounding medium in which the particles are placed and $\cosh\eta_0 = a/D$. In SP physics usually the infinite system of linear equations is truncated at a sufficiently big value of index n, afterwards the determinant of the truncated system is set equal to zero. Further, $\varepsilon(\omega)$ is found as the root of the obtained equation, which allows using the experimental data for $\varepsilon(\omega)$ [18] to find the SP frequencies of the longitudinal and transversal oscillation modes. In Fig. 1 the charge displacement for optically active longitudinal and transversal in-phase oscillations are shown.

As shown the frequencies of first few surface modes are found to converge and to be independent of truncation index n, provided that it is large enough [9]. Obviously, the larger the size of the truncated system of equations is, the more precise the results are. Therefore, to obtain a reliable value of the SP frequency the numerical solution of the system of equations of increasing size requires time-consuming calculations.

2 Continuous-fraction method

The analysis of three term recursive relations like (1) by use of continuous fractions is well known in the theory of special functions [19]. It turns out that the representation of a recursive relation in the form of a continuous fraction provides very rapid convergence [20], allowing us to sufficiently reduce the computational time. Below we apply the continuous-fraction approach to the set of (1) and show that it makes possible to reduce sufficiently the computational time. This circumstance allows interpreting existing experimental data and investigating theoretically the case of almost touching particles as well.

For convenience we introduce the following substitution in (1)

$$
\left[\varepsilon_m\cosh\left(n+\frac{1}{2}\right)\eta_0+\varepsilon(\omega)\sinh\left(n+\frac{1}{2}\right)\eta_0\right]A_n=F_n.
\tag{2}
$$

Then the initial system acquires a form close to Legendre polynomial recurrent relations and more convenient for further analysis

$$n F_{n-1} - (2n+1)\cosh\eta_0 \times \left[1 + \frac{1-x}{2n+1}\frac{\tanh\eta_0 \tanh(n+\frac{1}{2})\eta_0}{1 + x\tanh(n+\frac{1}{2})\eta_0}\right] \times F_n + (n+1)\,F_{n+1} = 0, \tag{3}$$

where $x = \varepsilon(\omega)/\varepsilon_m$. When $n \to \infty$, the factor in square brackets tends to unity, and the formula (3) becomes the Legendre polynomial recurrent relations of the argument $\cosh\eta_0$, i.e. $P_n(\cosh\eta_0)$. Further, we introduce the following notations for brevity

$$\alpha_n = \frac{1-x}{2n+1}\frac{\tanh\eta_0 \tanh(n+\frac{1}{2})\eta_0}{1 + x\tanh(n+\frac{1}{2})\eta_0}, \quad \frac{F_{n-1}}{F_n} = b_{n-1}, \quad \frac{2n+1}{n}\cosh\eta_0\,(1+\alpha_n) = p_n, \quad \frac{n+1}{n} = q_n. \tag{4}$$

For the further truncation at certain $n = N$ the (3), using (4), can be presented as the following continuous fraction:

$$b_{n-1} = p_n - \frac{q_n}{b_n}, \tag{5}$$

with the boundary condition

$$b_0 = \frac{1}{(1+\alpha_0)\cosh\eta_0}. \tag{6}$$

In order to perform an iterative process in (5) it is more convenient to invert the numbering of b_n, i.e. to start from N. Therefore we introduce new variables a_n instead of b_n according to

$$b_n = a_{N-n}, \qquad a_n = b_{N-n},$$
$$a_{N-n+1} = p_n - \frac{q_n}{a_{N-n}}, \quad N - n = m,$$

and hereby obtain a new recursive equation,

$$a_{m+1} = p_{N-m} - \frac{q_{N-m}}{a_m}, \qquad a_N = \frac{1}{(1+\alpha_0)\cosh\eta_0}. \tag{7}$$

The number N denotes the order of iterations that should be performed to solve (7). Since for $n \to \infty$ (3) coincides with the recurrent relation for the Legendre polynomials $P_n(x)$ it could be expected that for sufficiently big N one can set $a_0 = P_N(\cosh\eta_0)/P_{N+1}(\cosh\eta_0)$. However, the calculations show that the final result is independent of the value of a_0 already for $N = 30$, which allows us to choose any a_0, for example $a_0 = 1$. Such stability demonstrates the effectiveness of the introduced approach.

Performing the iteration procedure starting from $a_0 = 1$ and setting a_N according to (7) we can obtain an equation for $x = \varepsilon(\omega)/\varepsilon_m$. The most suitable way of solving the equation with respect to x is the graphical method. We solve the equation of a form $f(x) = 0$ numerically by plotting the curve $y = f(x)$ and determining the x-coordinates of intersection points of the curve and the X-axis, that is, the solutions of $f(\varepsilon(\omega)/\varepsilon_m) = 0$. The root $\varepsilon(\omega)/\varepsilon_m = -2$ gives the value of SP resonance frequency in case of infinite separation (isolated nanosphere) [21]. To obtain the values ω_{sp} of interacting nanospheres we have to choose the ones with the x-coordinate smaller than -2 since only they give the observed red-shift. It is interesting to mention that our calculation gives only one such root. The numerical calculation shows that it is quite enough to limit ourselves to $N = 50$, since any further increase of N does not influence the value of the root. This circumstance justifies the statement made above on the rapid convergence of the iteration procedure, which, contrary to known computational methods for ω_{sp}, actually allows almost immediate numerical solution of (7).

3 SP frequencies of almost touching small spheres

We start from the case of small enough spherical pairs so that the retardation effects can be neglected. First we compare our results (see Fig. 2, solid lines) with those obtained by Shmeits and Dambly (Fig. 2, squares) [10], where the dielectric function of the metal is chosen in the form $\varepsilon(\omega) = 1 - (\omega_p/\omega)^2$ (note that this dependence is appropriate for alkali metals). In this figure the dependence of dimensionless SP resonance frequency ω_{sp}/ω_p on dimensionless reciprocal center-to-center interparticle distance R/a (ω_p is the

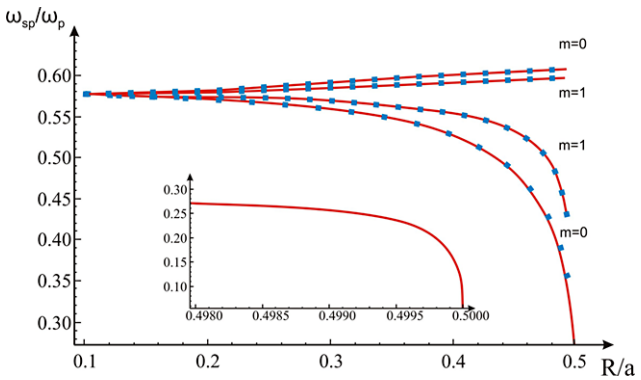

Fig. 2 Dimensionless SP frequency of coupled nanospheres ω_{sp}/ω_p vs. radius-to-interparticle distance ratio R/a for in-phase (*lower curves*) and counter-phase (*upper curves*) longitudinal plasmon oscillations. The curves with $m = 0$ correspond to dipole oscillations and the curves with $m = 1$ describe quadrupole oscillations. Simultaneously the upper curve with $m = 1$ corresponds to the in-phase transversal dipole oscillations and the lower one with $m = 1$ to the counter-phase transversal dipole oscillations. The *solid lines* represent the current study and the *squares* are the results of Shmeits and Dambly [10]. The part of the plot covering extremely small gaps for in-phase oscillations ($m = 0$) is shown separately in the *inset*

plasma oscillation frequency of bulk metal) for longitudinal in-phase and counter-phase dipole ($m = 0$) and quadrupole ($m = 1$) modes are shown.

As can be seen the curves representing our approach coincide with those obtained in [10] for the whole range of interparticle distances up to $a = 1.014D$. The comparison of our results with more recent numerical calculations for much smaller interparticle distances (see inset in Fig. 2) of [5] again shows perfect agreement. Naturally the approach developed in Sect. 2 is not applicable for extremely small interparticle distances comparable to atomic size, when various quantum effects such as nonlocality of the surface charge distribution contribute [15]. The advantage of our technique lies in its simplicity, which allows one to avoid time-consuming numerical calculations. Indeed, if we limit N for example to 50, the number of iterations to be performed in (7) is 50, whereas using of the procedures developed in [10] and [5] require solving of thousands of equations.

The case of the quadrupole mode can be considered in the same manner described above for the dipole oscillations. The following system of equations with respect to unknown expansion coefficients B_n for the quadrupole mode in bispherical coordinates is derived:

$$
\begin{aligned}
&(n-1)\left[\varepsilon_m \cosh\left(n-\frac{1}{2}\right)\eta_0\right.\\
&\left.+\varepsilon(\omega)\sinh\left(n-\frac{1}{2}\right)\eta_0\right]B_{n-1}\\
&-[\varepsilon_m-\varepsilon(\omega)]\sinh\eta_0\sinh\left(n+\frac{1}{2}\right)\eta_0 B_n\\
&-(2n+1)\left[\varepsilon_m\cosh\left(n+\frac{1}{2}\right)\eta_0\right.\\
&\left.+\varepsilon(\omega)\sinh\left(n+\frac{1}{2}\right)\eta_0\right]\cosh\eta_0 B_n\\
&+(n+2)\left[\varepsilon_m\cosh\left(n+\frac{3}{2}\right)\eta_0\right.\\
&\left.+\varepsilon(\omega)\sinh\left(n+\frac{3}{2}\right)\eta_0\right]B_{n+1}=0.
\end{aligned}
\tag{8}
$$

This recurrent relation after the following substitution analogous to (2),

$$
\left[\varepsilon_m\cosh\left(n+\frac{1}{2}\right)\eta_0+\varepsilon(\omega)\sinh\left(n+\frac{1}{2}\right)\eta_0\right]B_n=G_n
$$

acquire a form resembling the recurrent relation for associated Legendre functions $P_n^1(\cosh\eta_0)$ and describes the antisymmetric oscillations. The transition to the symmetric ones needs the substitution of $\cosh(x) \rightleftarrows \sinh(x)$. As can be seen from Fig. 2 the results obtained by both methods for the quadrupole mode again are practically indistinguishable.

We have also considered the transversal oscillations, for which the recurrent relations in the general case of different spheres are obtained in [12]. Setting the radii and dielectric functions of the materials of two spheres equal to each other, we have obtained recurrent relations fully coinciding with (8) therefore the corresponding graphs are not presented. Thus, the upper curve in Fig. 2 corresponding to $m = 1$ describes the behavior of in-phase transversal dipole mode as well.

The other approach to the calculation of SP frequencies of coupled small nanospheres is presented by Jain et al. [13], where calculation of the plasmon extinction efficiency of a pair of Au nanospheres with diameter 10 nm in water (refractive index $n = 1.33$) was performed by use of the discrete dipole approximation (DDA) [22]. Each sphere was represented by a $30 \times 30 \times 30$ cubic array of dipoles, corresponding to an interdipole spacing of 0.33 nm. The fractional plasmon shift $\Delta\lambda/\lambda_0$ (λ_0 is the single-particle SP wavelength) versus the ratio g/D was calculated, where g is the edge-to-edge gap. We calculated $\Delta\lambda/\lambda_0$ using equations (6) and (7) and experimental data of $\varepsilon(\omega)$ [18] for the same values of g and other parameters of the system considered in [13]. In Fig. 3 for the comparison we present the results of both calculations.

As can be seen from Fig. 3 a discrepancy between our calculation and DDA simulation arises for the gaps less than the sphere diameter and the absolute difference increases with decrease of the separation. As to the relative difference in the fractional red-shift for the gap values less than the radius it remains constant near the value of 20%. Thus for the adequate description of nearly touching spheres in the frame of DDA apparently much larger number of discretization points must be involved, which, however, will increase substantially the computing time [8]. It would be interesting to carry out new measurements with sufficiently small pair of nearly touching nanospheres in order to observe the actual rate of the red-shift of SP resonance wavelengths.

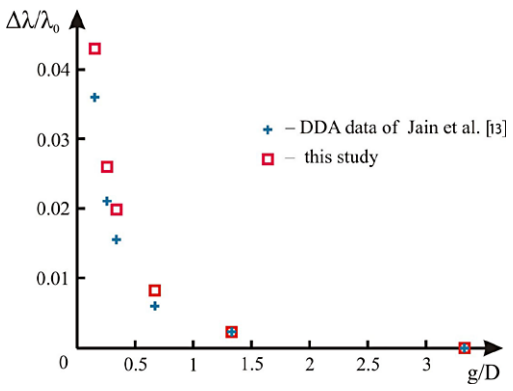

Fig. 3 Fractional *red*-shift of longitudinal SP resonance wavelength of coupled 10 nm Au spheres vs. g/D calculated by the DDA [13] and continuous-fraction method for the same values of interparticle gaps

We mention that in [11] the SP frequencies of the pair of 10 nm spheres are calculated using a finite elements method and as can be seen from Figs. 8 and 10 of [11] the results for retarded and nonretarded cases for center-to-center interparticle distances starting from 2 nm and larger are the same.

4 SP frequencies of large nanopairs

In some experiments on SP frequencies of coupled nanoparticles the results are obtained for relatively large particles with diameters over 40 nm [1–3]. Under these conditions the influence of the retardation effects must be accounted for, since the diameter of the sphere in the pair is of the order of SP radiation wavelength: $D \sim \lambda_{sp}/2\pi$. In order to calculate the SP frequencies of coupled spheres accounting for retardation effects, Maxwell equations along with corresponding boundary conditions are solved numerically [23]. Other approaches to account for the retardation effects are based on the discrete dipole approximation (DDA) [22, 24] and T-matrix method [25] that are widely used in MNP optics [1–3, 23]. It should be mentioned, however, that for the calculation of SP frequencies of coupled spheres all these methods require substantial computational time.

In this section we apply our calculational technique to the case investigated experimentally in [2], where the SP frequencies of the systems of two strongly coupled identical Au spheres with diameters of 42 nm and 87 nm are measured. To extend our approach developed in Sect. 3 to this experimental situation one has to include the contribution arising from the retardation effects. For the particles investigated this contribution is not large and can be accounted for as a small correction in the following manner.

It is well known that the poles of the scattering amplitude of Mie's solution [21] determine the SP frequency of an isolated sphere with taking retardation exactly into account. We start from the case of two identical noninteracting spheres and consider the effect of retardation in each of them. Following [26] and expanding Bessel functions in the denominator of the scattering amplitude with respect to the argument $\omega R/c$ (c is the speed of light) and keeping only the first two terms the equation for the SP frequency of each sphere can be obtained

$$\varepsilon(\omega) + 2\left(1 + \frac{6}{5}\frac{\varepsilon_m \omega^2}{c^2}R^2\right)\varepsilon_m = 0. \tag{9}$$

The second term in parentheses is the first correction due to the retardation and is of order of $\mu = (2\pi D/\lambda_{sp})^2$. Note that for $D = 42$ nm the values of $\mu \approx 0.18$ and for $D = 87$ nm, $\mu \approx 0.83$. In order to check the validity of this approximation we compared SP frequencies of an isolated sphere calculated numerically [11] with the results following from (9) (see Table 1) as well as with recent experimental data [27].

As can be seen from the Table 1. the difference in SP frequencies between the results of [11] and those following from (9) is less than 1.3% up to $D = 75$ nm indicating a sufficiently wide range of applicability of (9). Moreover even for 90 nm spheres the deviation of the results obtained with (9) from experimental data [27] (Au spheres in water solution) does not exceed 2%.

In order to investigate the influence of the retardation on the SP frequency of interacting spheres we perform the following substitution in (3)

$$\frac{\varepsilon(\omega)}{\varepsilon_m} \to \frac{\varepsilon(\omega)}{\varepsilon_m} + \frac{12}{5}\frac{\varepsilon_m \omega^2}{c^2}R^2. \tag{10}$$

The substitution (10) means that we account for retardation effects within each of the spheres, neglecting it in the electromagnetic interaction between the spheres, which is justified for not very small interparticle distances. As to the system of two almost touching spheres, physically it represents unified structure with doubled size where the retardation effects in the interparticle interaction become important as well and must be involved. This kind of size effect is also revealed in the radiation damping, leading to the increase of damping rate with increase of a system volume [28]. For the same reason the numerically calculated values of radiation damping rate demonstrate a sharp increase in the case of interparticle gaps less than $2D$ for nanospheres with $D = 80$ nm [29].

We compare the results obtained according to (7) and (10) for longitudinal SP oscillations (along the interparticle axis) with the available experimental data. The results of our calculations (using the data of [18]) as well as the experimental data and T-matrix numerical calculations of [2] for 42 nm pairs are presented in Fig. 4.

Since the best agreement between T-matrix calculations and experiment [2] was obtained for the refractive index of host media $n = 1.6$, we use this value in our calculations. As can be seen from Fig. 4 our method provides good agreement with experimental data and T-matrix calculations. We

Table 1 SP resonance frequencies of isolated Au spheres of six different radii calculated numerically by applying the discretization procedure [11] and (9)

D (nm)	1	10	25	50	75	85
ω_{sp} (eV), [11]	2.3823	2.38	2.36	2.29	2.18	Not available
ω_{sp} (eV), (9)	2.3823	2.379	2.358	2.294	2.209	2.172

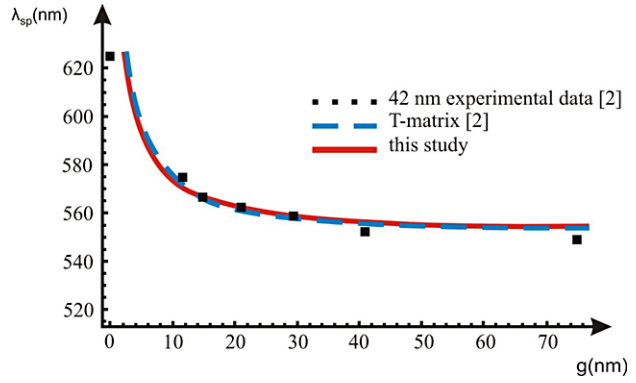

Fig. 4 SP resonance wavelength of 42 nm coupled Au spheres vs. interparticle gap. The data of [2]: *full squares*—experimental data, *dashed line*—T-matrix calculation. The *solid line* is the result of calculations based on (7) and (10)

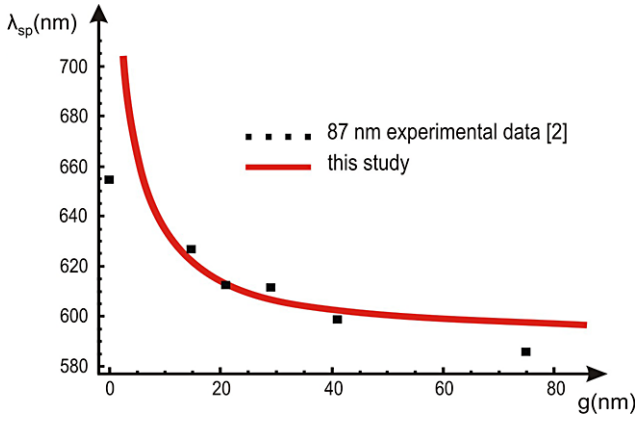

Fig. 5 SP resonance wavelength of 87 nm coupled Au spheres vs. interparticle gap. *Full squares* are experimental data of [2], the *solid line* is the result of calculations based on (7) and (10)

note that the results of a T-matrix simulation for 40 nm pairs [1] with other value of the refractive index $n = 1.5$ also coincide with the experimental data of [2].

It is interesting to mention that the coincidence between all theoretical results for longitudinal SP modes and measured values takes place despite the fact that in measured spectra the perpendicular mode was present as well. We attribute this to the large spectral separation between the transversal and longitudinal modes as well as to the low sensitivity of the transversal mode with respect to the center-to-center interparticle distance (see Fig. 2).

It is easy to see (Fig. 4) that in the gap region of $g =$ 5–20 nm for 42 nm pairs the largest deviation of theoretical values of g from the experimental data takes place at SP wavelength $\lambda_{sp} \approx 575$ nm and is equal to $|\Delta g| \approx 3$ nm. This gives for the spatial accuracy of nanoruler $\rho = g/|\Delta g|$ the lower limit $\rho \geq 6$.

Let us turn to the 87 nm rulers, for which the SP frequency dependence on interparticle gap, as the experiment shows, is less steep and which are interesting for biological applications in the measurements of larger distances. The results of calculations for a 87 nm ruler imbedded in the host media with $n = 1.6$ based on (7) with substitution (10) and the experimental data [2] are presented in Fig. 5.

As can be seen from Fig. 5 for the gap range $g =$ 10–40 nm there is a good agreement between experimental data and the results of our calculations of longitudinal SP mode. The disagreement of the calculated and measured values beyond the mentioned gap region for both smaller as well as larger values is obviously conditioned by the approximate treatment of retardation. We note here that the T-matrix simulations [1, 2] do not match the experimental data for pairs of the spheres with $D = 80$ nm and 87 nm.

For 87 nm pairs (see Fig. 5) in the gap region of $g =$ 10–40 nm, analogous to the case of 42 nm spheres, one can obtain $|\Delta g| \approx 4$ nm at $\lambda_{sp} \approx 620$ nm, and accordingly for the spatial accuracy $\rho \geq 5$.

5 Conclusion

A semianalytical approach to the SP resonance frequency calculation in a system of two nearly touching spheres is developed. In contrast to widely used simulation methods applying a discretization procedure like DDA or T-matrix method, our approach is based on the analytical theory of continuous fraction. The proposed method leads to an iteration procedure with rapid convergence and by that reduces both the calculational errors and computational time. Since the method does not require extended computer facilities and permits quick and efficient processing of experimental data it can be considered as a theoretical basis for a plasmon nanoruler in the region of extremely small interparticle gaps. The advantage of our technique is demonstrated for the smallest interparticle distances (nearly touching nanoparticles) never considered analytically before.

It turns out that for small particles with $D = 10$ nm our calculations for the fractional red-shift at smaller gaps give larger values as compared to earlier published results obtained in the frame of DDA [13]. In addition, it is revealed that the difference in red-shifts grows with decrease of interparticle gap.

In order to expand the developed theory to the case of larger particles in the pairs and compare the results with existing experimental data the influence of retardation effects on SP resonances is accounted for as well. It is shown that the effect of the finiteness of the speed of light can be properly handled in the frame of the approach developed here. The ranges of interparticle gaps valuable for biological applications are determined and the lower limits of spatial resolution of 42 nm and 87 nm rulers are identified.

For pairs of larger particles with $D = 80$ nm (not shown here) and 87 nm, in contrast to T-matrix simulation [1, 2], our calculations in the gap range of $g =$ 10–40 nm describe the experimental data with good accuracy.

References

1. Q.-H. Wei, K.-H. Su, S. Durant, X. Zhang, Nano Lett. **4**, 1067 (2004)
2. B.M. Reinhard, M. Siu, H. Agarwal, A.P. Alivisatos, J. Liphardt, Nano Lett. **5**, 2246 (2005)
3. T. Atay, J.-H. Song, A.V. Nurmikko, Nano Lett. **4**, 1627 (2004)
4. H. Xu, M. Käll, Phys. Rev. Lett. **89**, 246802 (2002)
5. P. Nordlander, C. Oubre, E. Prodan, K. Li, M.I. Stockman, Nano Lett. **4**, 899 (2004)
6. F.J. Garcia de Abajo, Phys. Rev. B **60**, 6086 (1999)
7. I. Romero, J. Aizpurua, G.W. Bryant, F.J. García de Abajo, Opt. Express **14**, 9988 (2006)
8. V. Myroshnychenko, J. Rodrıguez-Fernandez, I. Pastoriza-Santos, A.M. Funston, C. Novo, P. Mulvaney, L.M. Liz-Marzan, F.J. Garcıa de Abajo, Chem. Soc. Rev. **37**, 1792 (2008)
9. R. Ruppin, Phys. Rev. B **26**, 3440 (1982)
10. M. Shmeits, L. Dambly, Phys. Rev. B **44**, 12706 (1991)
11. U. Hohenester, J. Krenn, Phys. Rev. B **72**, 195429 (2005)
12. P. Chu, D. Mills, Phys. Rev. B **77**, 045416 (2008)
13. P.K. Jain, W. Huang, M.A. El-Sayed, Nano Lett. **7**, 2080 (2007)
14. S.A. Maier, M.L. Brongersma, P.G. Kik, H.A. Atwater, Phys. Rev. B **65**, 193408 (2002)
15. F.J. Garcia de Abajo, J. Phys. Chem. C **112**, 17983 (2008)
16. P. Johansson, H. Xu, M. Käll, Phys. Rev. B **75**, 035427 (2005)
17. M. Chergui, A. Melikyan, H. Minassian, J. Phys. Chem. C **113**, 6463 (2009)
18. P.B. Johnson, R.W. Christy, Phys. Rev. B **6**, 4370 (1972)
19. M. Abramowitz, A. Stegun, *Handbook of Mathematical Functions* (Dover, New York, 1964)
20. A.Ya. Khinchin, *Continued Fractions* (University of Chicago Press, Chicago, 1961)
21. U. Kreibig, M. Vollmer, *Optical Properties of Metal Clusters* (Springer, Berlin, 1995)
22. B.T. Draine, P.J. Flatau, J. Opt. Soc. Am. A **11**, 1491 (1994)
23. F.J. García de Abajo, A. Howie, Phys. Rev. B **65**, 115418 (2002)
24. K.L. Kelly, E. Coronado, L.L. Zhao, G.C. Schatz, J. Phys. Chem. B **107**, 668 (2003)
25. M.I. Mishchenko, L.D. Travis, A.A. Lacis, *Scattering, Absorption and Emission of Light by Small Particles* (Cambridge University Press, Cambridge, 2002)
26. C.F. Bohren, D.R. Huffman, *Absorption and Scattering of Light by Small Particles* (Wiley, New York, 1983)
27. P. Njoki, I. Lim, D. Mott, H. Park, B. Khan, S. Mishra, R. Sujakumar, J. Luo, C. Zhong, J. Phys. Chem. C **111**, 14664 (2007)
28. A. Melikyan, H. Minassian, Appl. Phys. B, Lasers Opt. **78**, 455 (2004)
29. C. Dahmen, B. Schmidt, G. von Plessen, Nano Lett. **7**, 318 (2007)